



A Fresh View of Global Atmosphere and Ionosphere from the Combined GNSS-RO (Radio Occultation) Constellations

Dong L. Wu

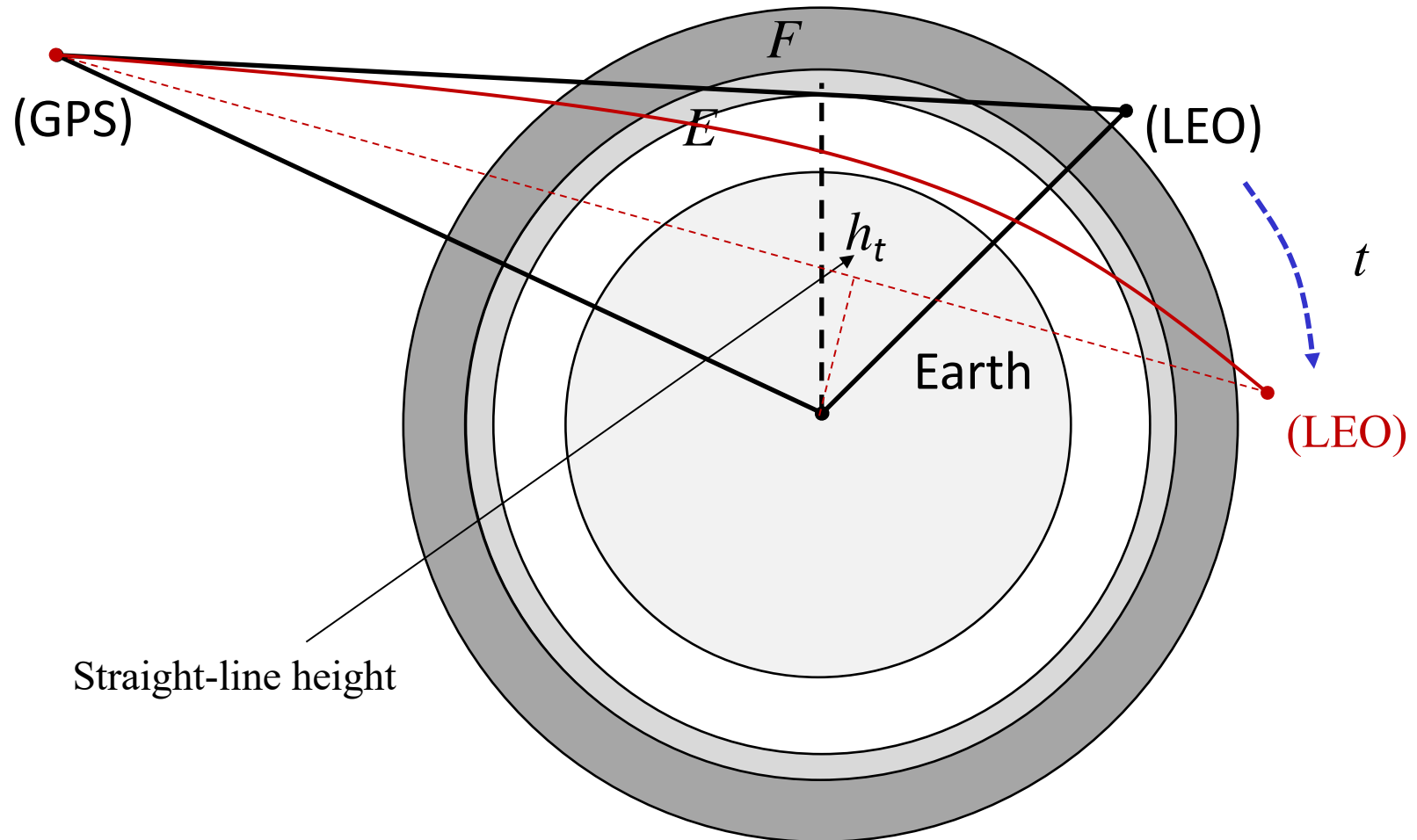
NASA Goddard Space Flight Center, Code 613

Acknowledgments:

- Contributions from Daniel Emmons, Nimalan Swarnalingam, Manisha Ganeshan, Jie Gong, Tyler Summers
- Fundings from NASA's Programs: Commercial Smallsat Data Acquisition (CSDA), GNSS Science Team, Living With Star (LWS), and Sun-Climate Research

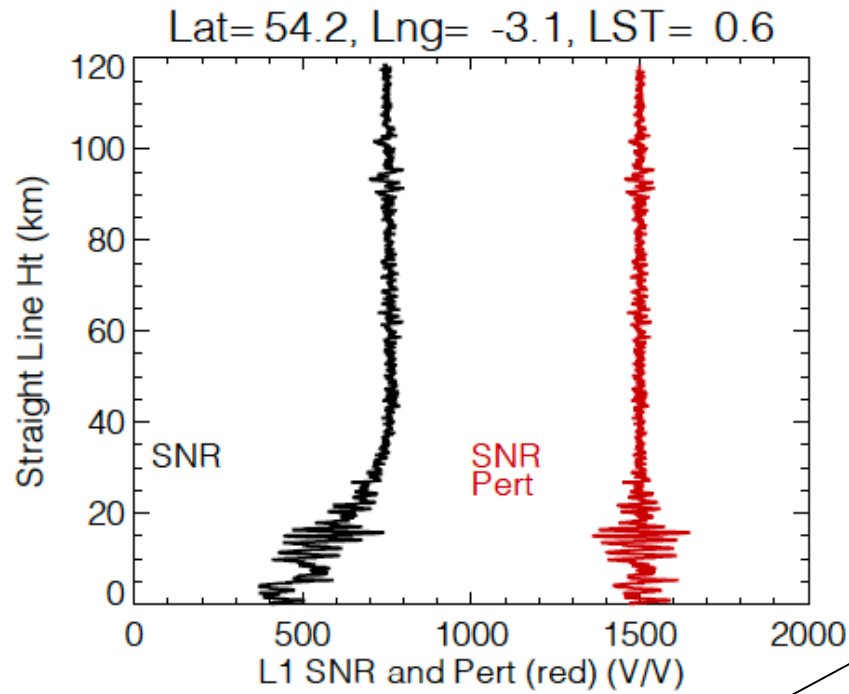


Global Navigation Satellite Systems (GNSS) Radio Occultation (RO)

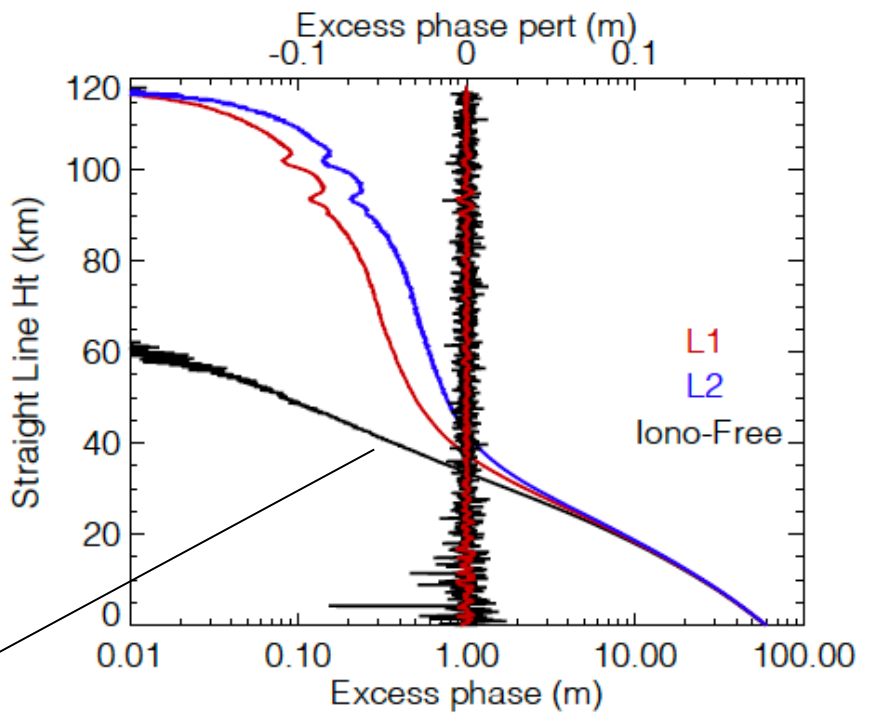




RO Amplitude

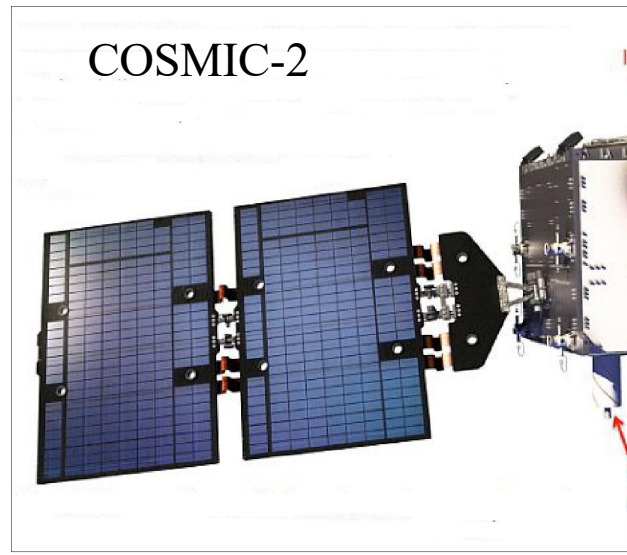


RO Excess Phase



$$N = (n - 1) \times 10^6 = 76.6 \frac{P}{T} + 3.73 \times 10^5 \frac{P_w}{T^2} - 4.03 \times 10^7 \frac{n_e}{f^2} + o(IWP, f^3, f^4)$$

Operation Research



POD
antenna

1 Hz

RO
antenna

1 Hz

50/100 Hz

GPS

POD hTEC

GPS

POD antennas (2x)

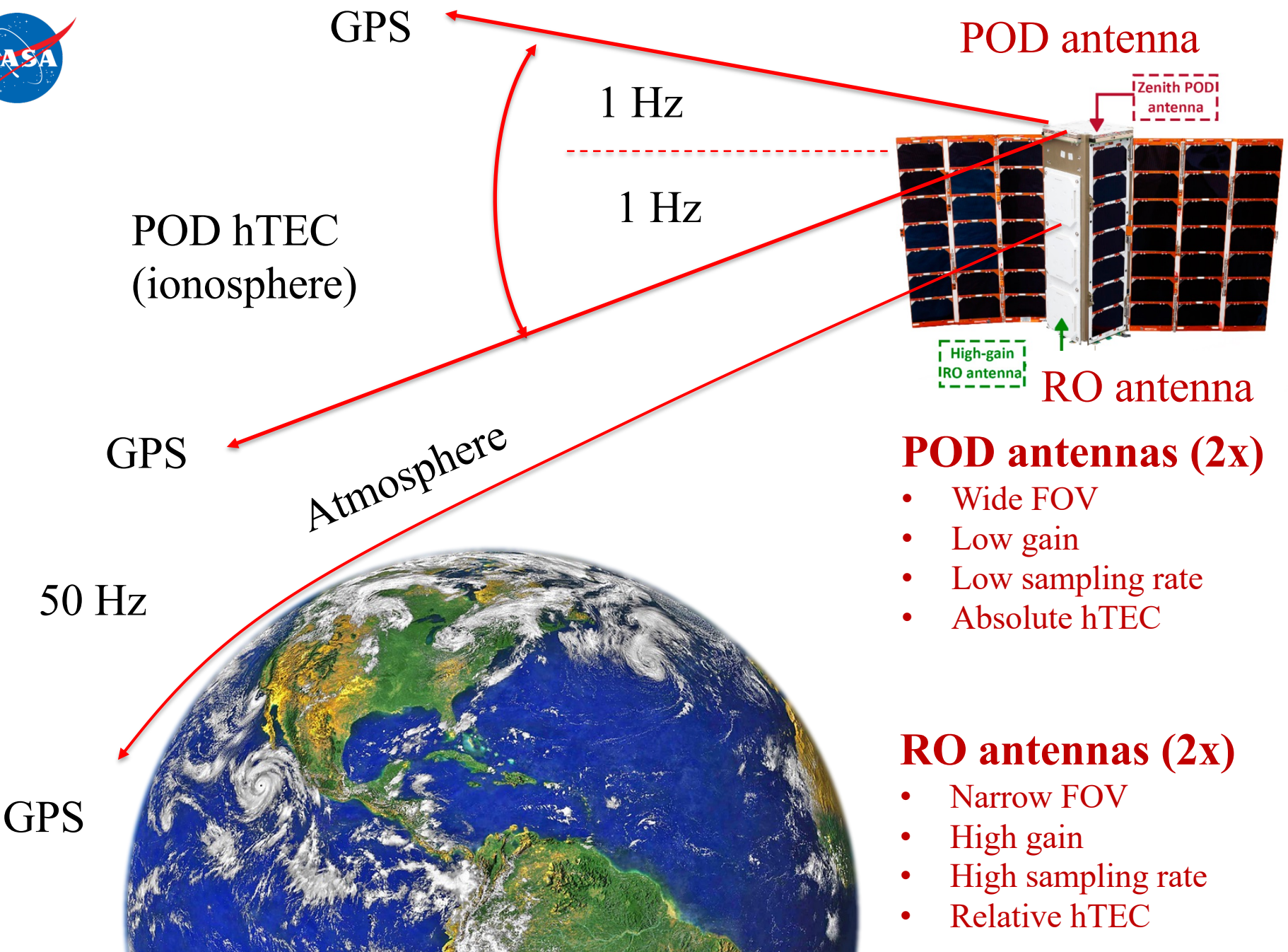
- Wide FOV
- Low gain
- Low sampling rate
- Absolute hTEC

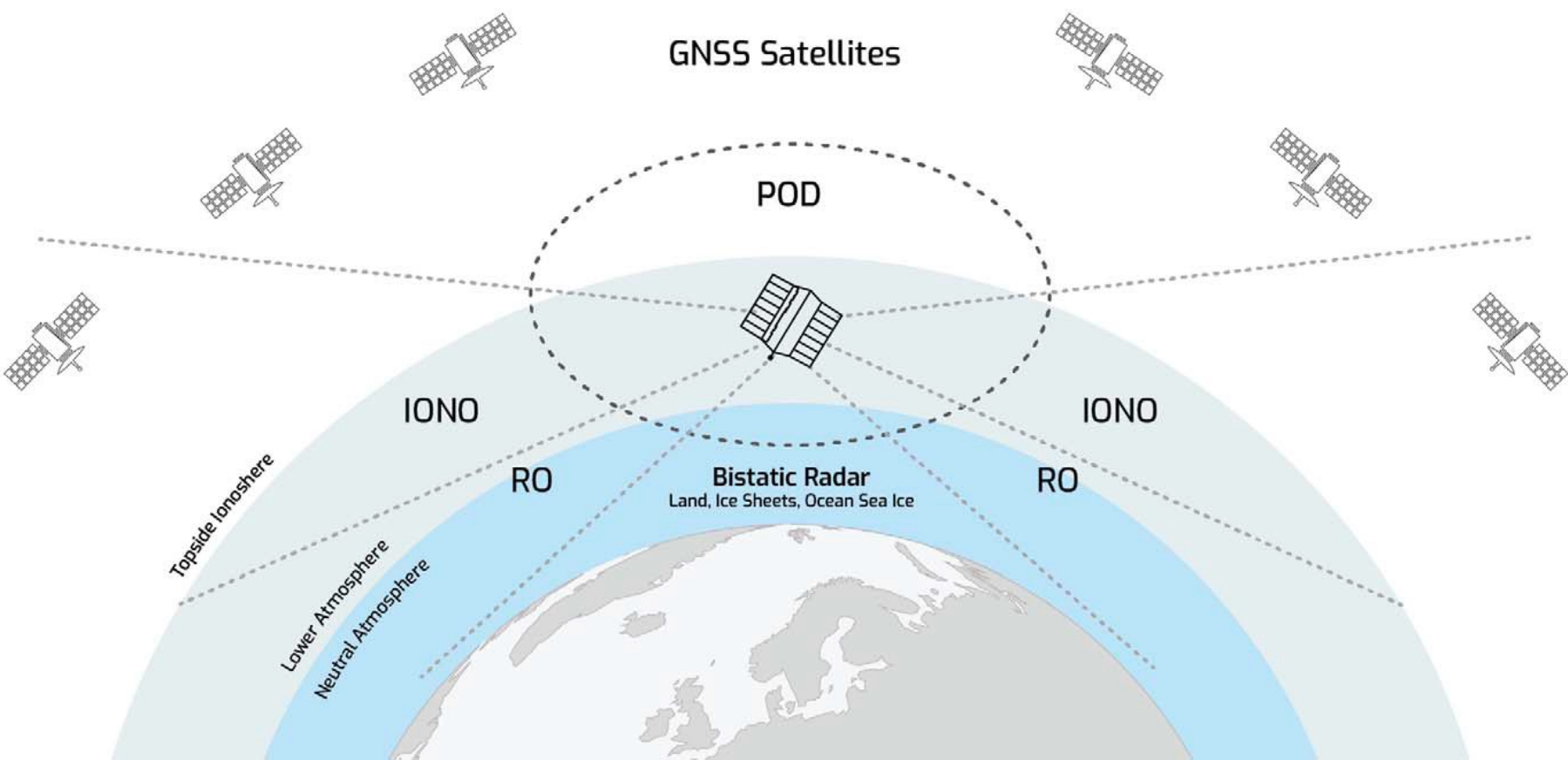
RO antennas (2x)

- Narrow FOV
- High gain
- High sampling rate
- Relative hTEC



GPS



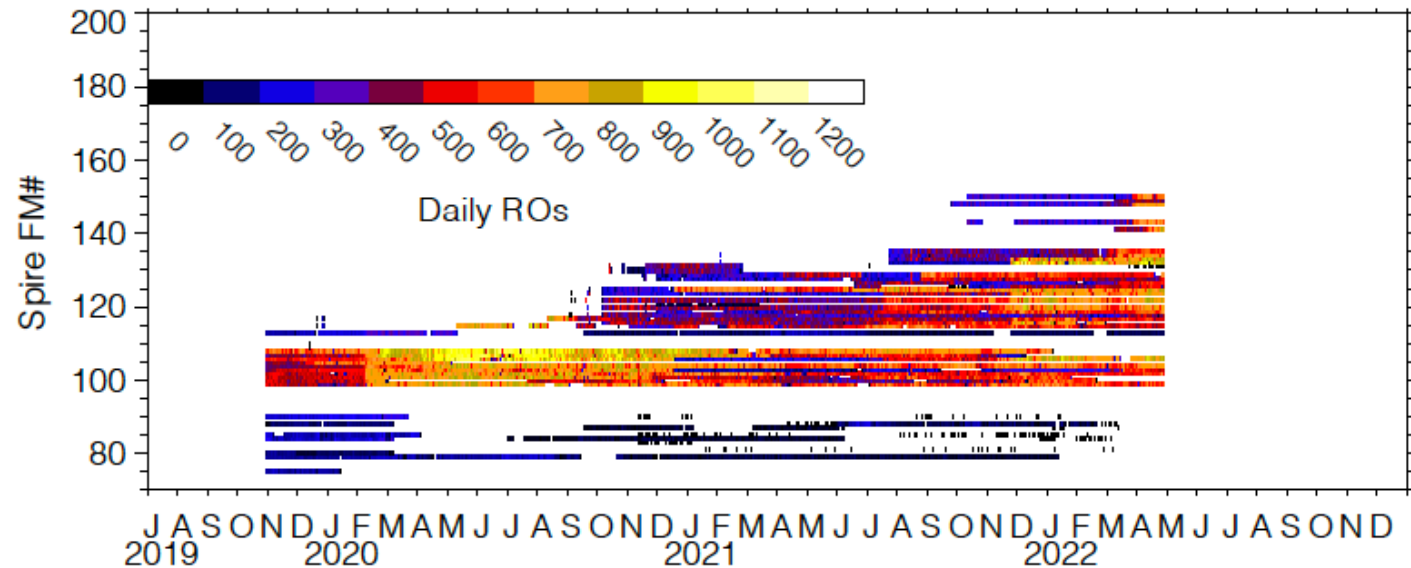


Angling et al. (2021)

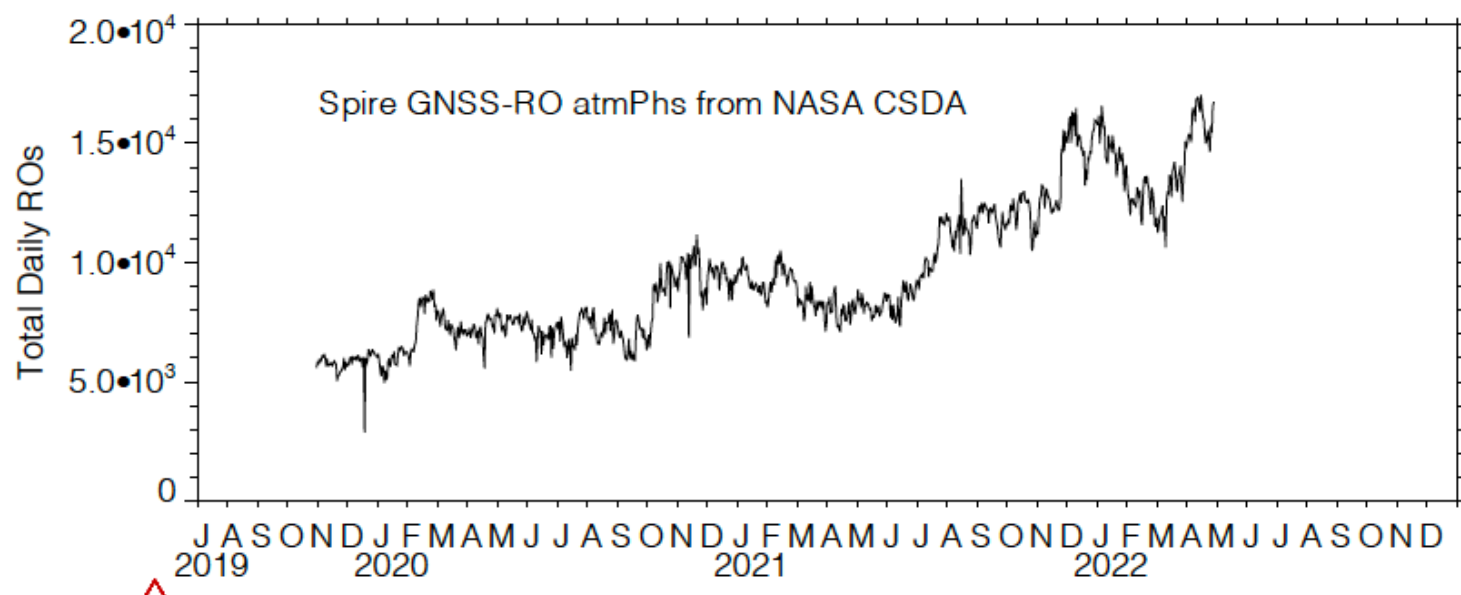


Spire Daily GNSS-RO Statistics (L1B: atmPhs)

By flight
model (FM)

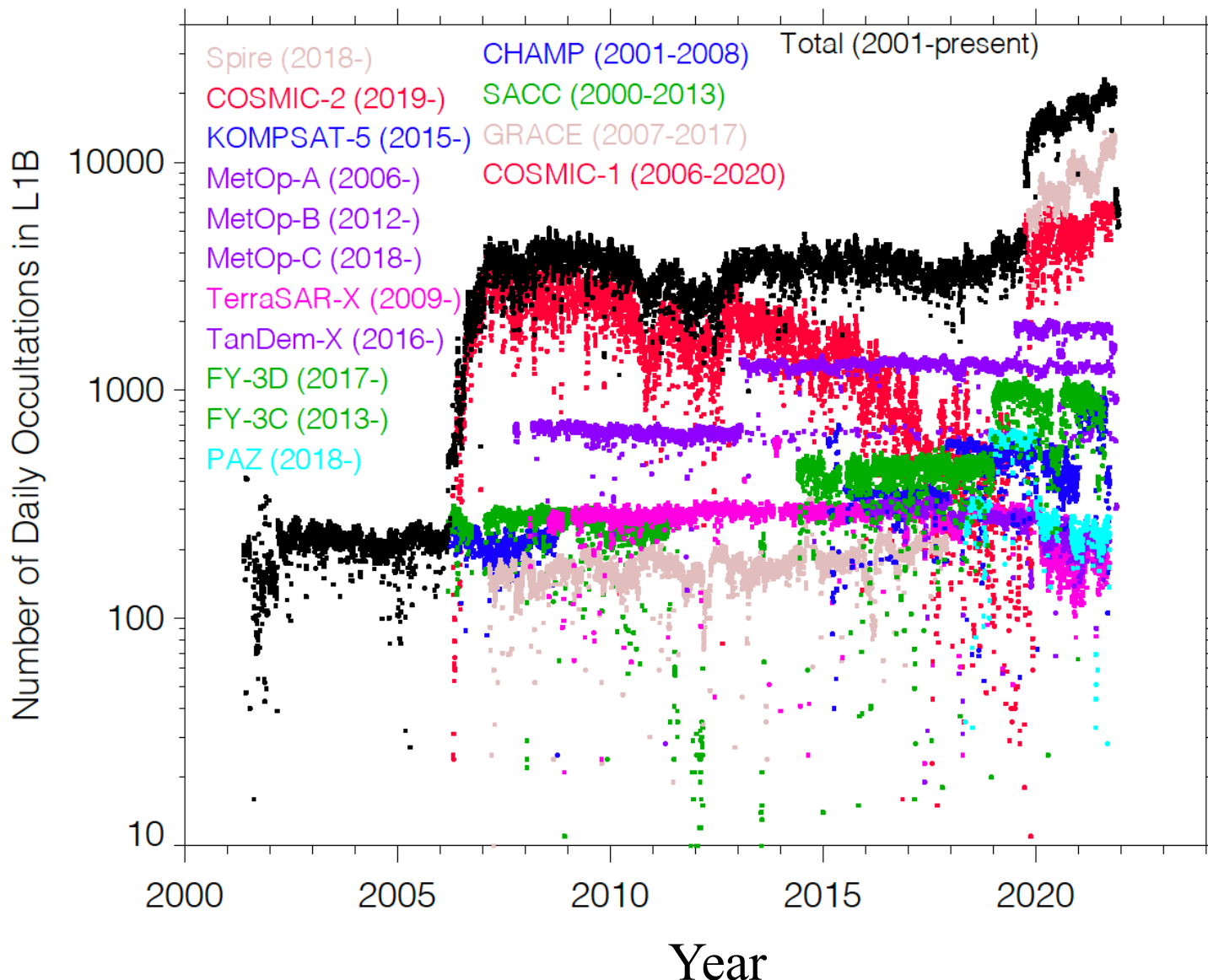


Total
daily
number





Daily RO Observations Since CHAMP (NASA-DLR)



Wu et al. (Remote Sensing, 2022a)



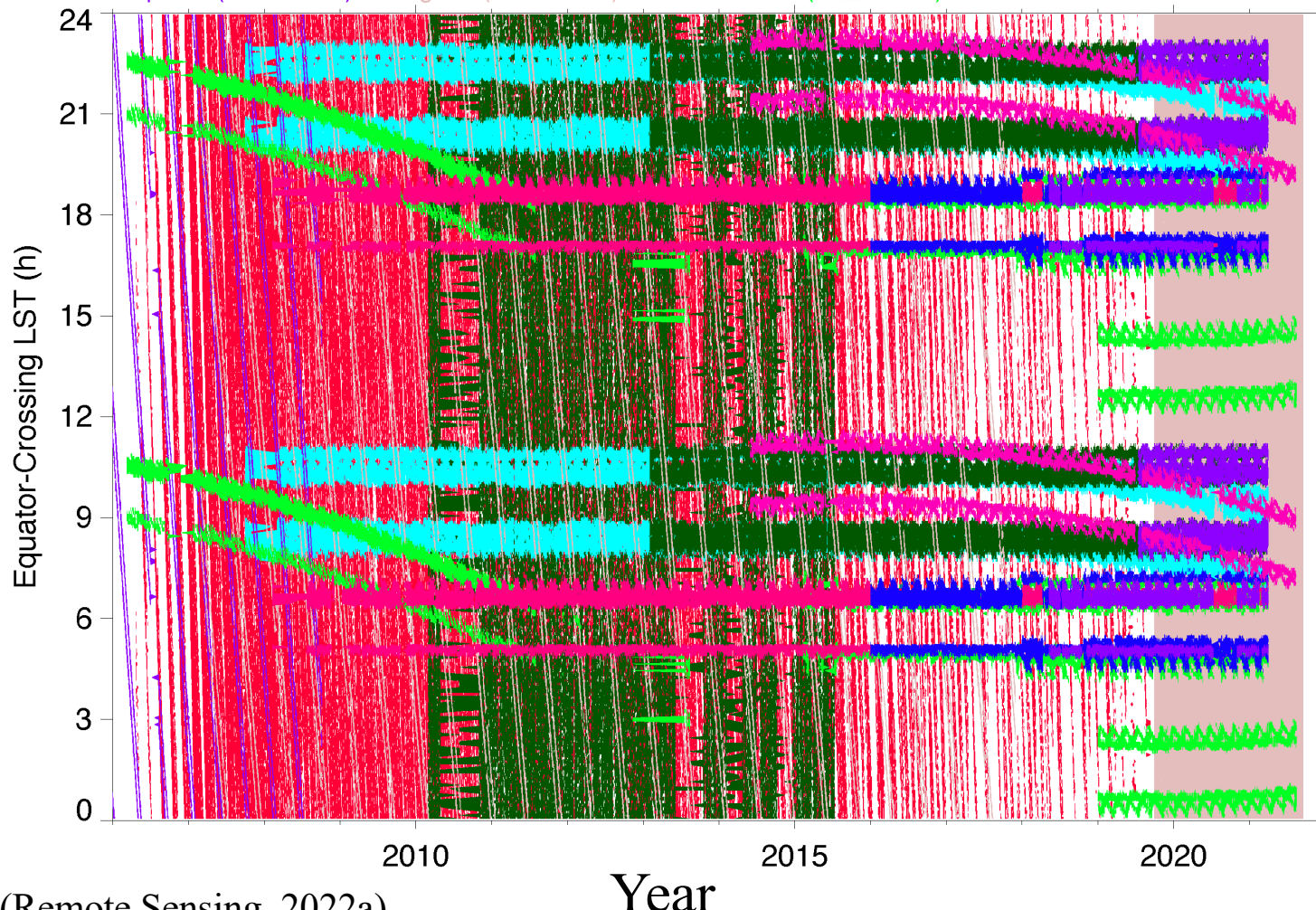
Local Time Sampling

COSMIC1-1 (2006-2018)
COSMIC1-2 (2006-2016)
COSMIC1-3 (2006-2010)
COSMIC1-4 (2006-2015)
COSMIC1-5 (2006-2017)
COSMIC1-6 (2006-2020)
champ2016(2001-2008)

COSMIC2-1 (2019-)
COSMIC2-2 (2019-)
COSMIC2-3 (2019-)
COSMIC2-4 (2019-)
COSMIC2-5 (2019-)
COSMIC2-6 (2019-)
grace(2007-2017)

cnois (2008-2015)
metopa2016 (2007-2015)
metopa (2016-)
metopb2016 (2013-2015)
metopb (2016-)
metopc (2018-)
sacc(2006-2013)

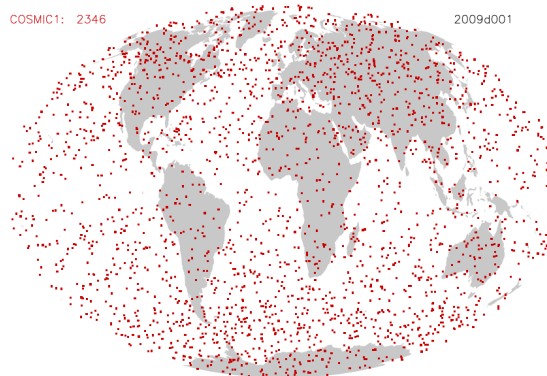
kompsat5 (2015-)
tsx (2008-)
tdx (2016-)
paz (2018-)
fy3c (2014-)
fy3d (2019-)



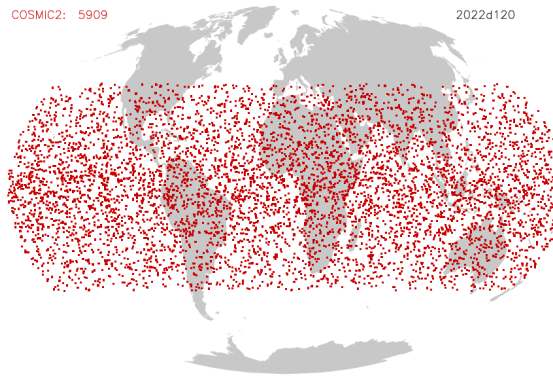


Daily Sampling Maps from GNSS RO

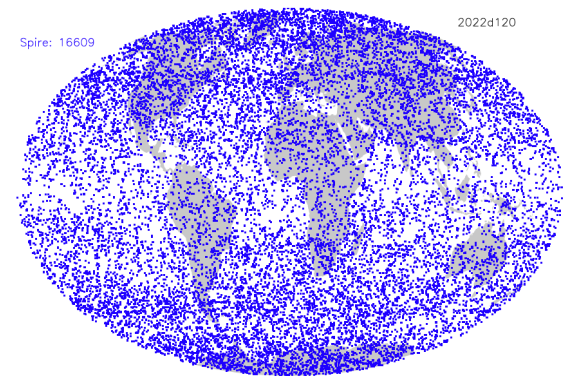
COSMIC-1
(2006-2020)



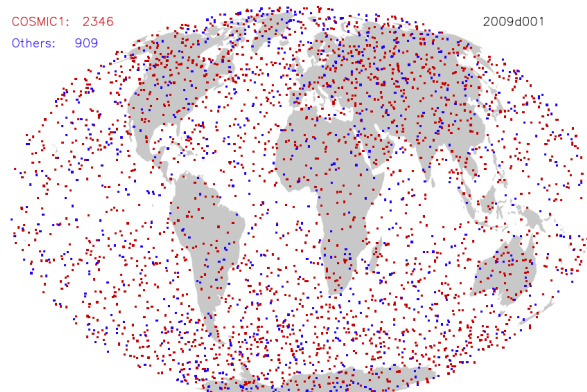
COSMIC-2
(2020-)



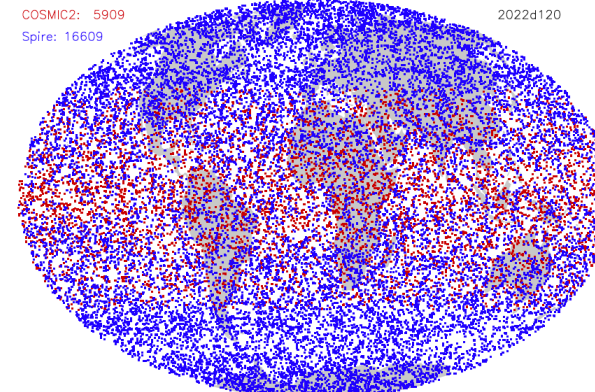
Spire
(2019-)



COSMIC-1 + Others (2009d001)



COSMIC-2 + Spire (2022d120)

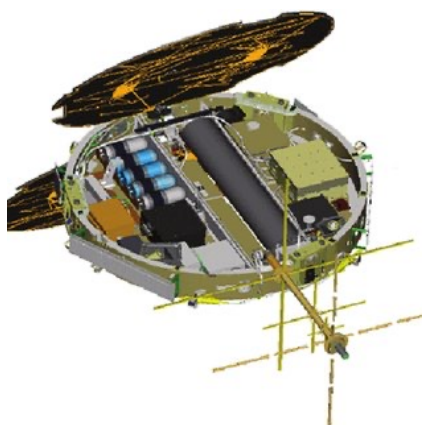




Comparisons of LEO Satellite Dimension and GNSS Tracking

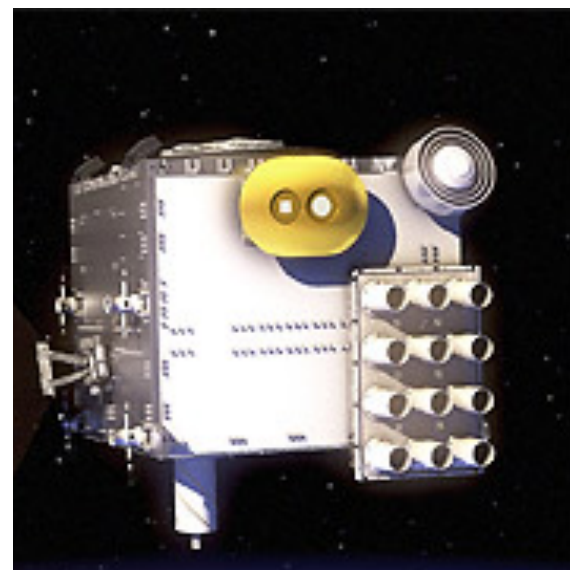
COSMIC-1

D = 100 cm
H = 18 cm



COSMIC-2

(L × W × H)
125 × 100 × 125 cm



Spire

(L × W × H)
10 × 10 × 30 cm



GNSS Tracking

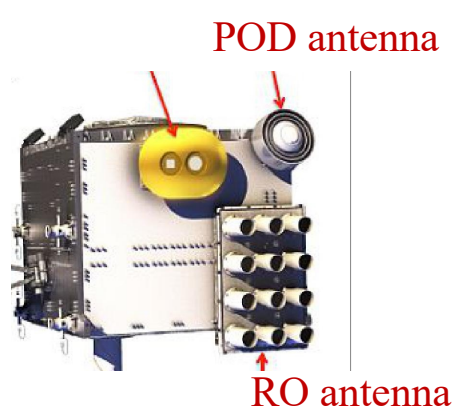
U.S. Navstar Global Positioning System (GPS)
Russia's GLObal NAVigation Satellite System (GLONASS) constellations
European Navigation Satellite System Galileo (Galileo)
Japanese Quasi Zenith Satellite System (QZSS).

COSMIC-1	COSMIC2	Spire
GPS	GPS, GLONASS	GPS, GLONASS, Galileo, QZSS



Sampling Comparisons of GNSS-RO and GNSS-POD

	RO Antennas (Atmos & D/E-Region)	POD Antennas (F-Region)		
	Total L1B	Ne	Total L1B	Ne
COSMIC-1 (Jan 1, 2008)	1,690	1,419	1,832	1,175
COSMIC-2 (Jan 1, 2022)	6,199	6,068	9,366	6,661
Spire (Jan 1, 2022)	15,900	15,756	18,433	5,960



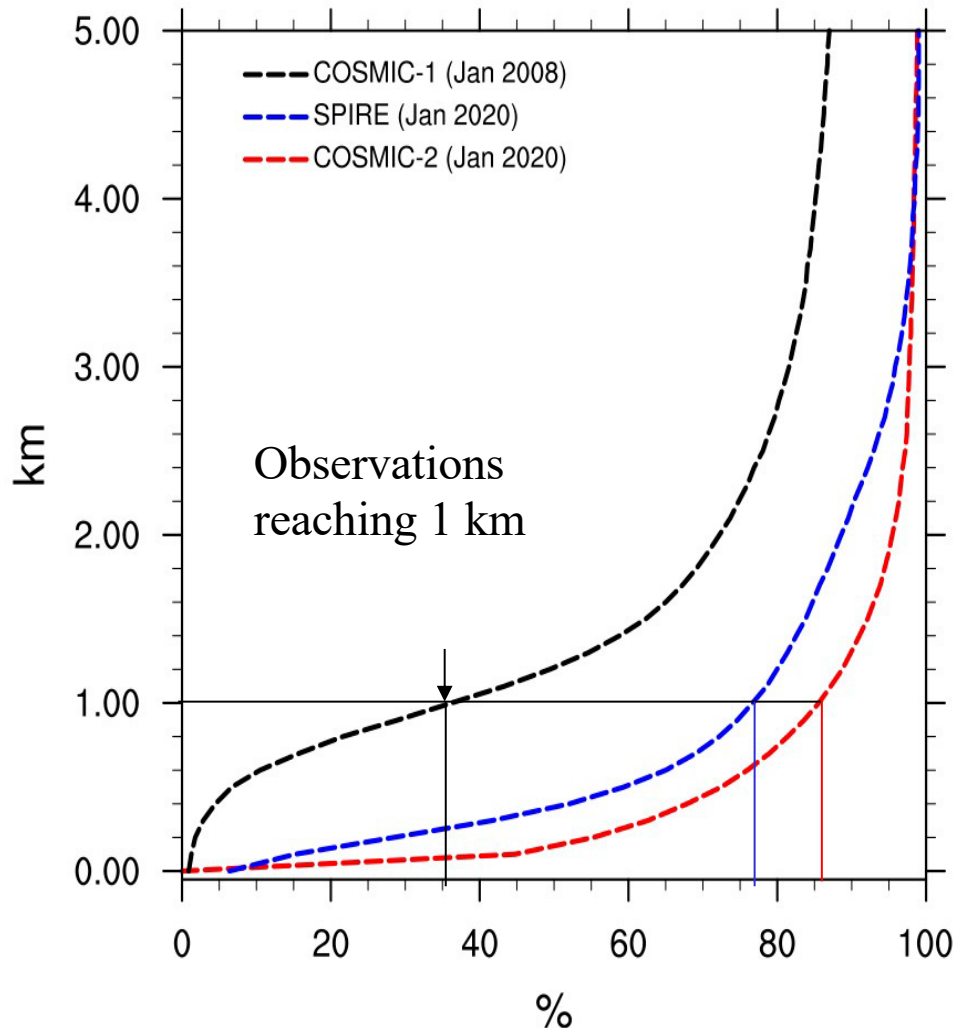


Atmospheric Sciences



Fraction of SPIRE RO observations reaching PBL (ocean & low, flat land only)

Percentage Observations: Tropics (Ocean+Low,Flat Land)



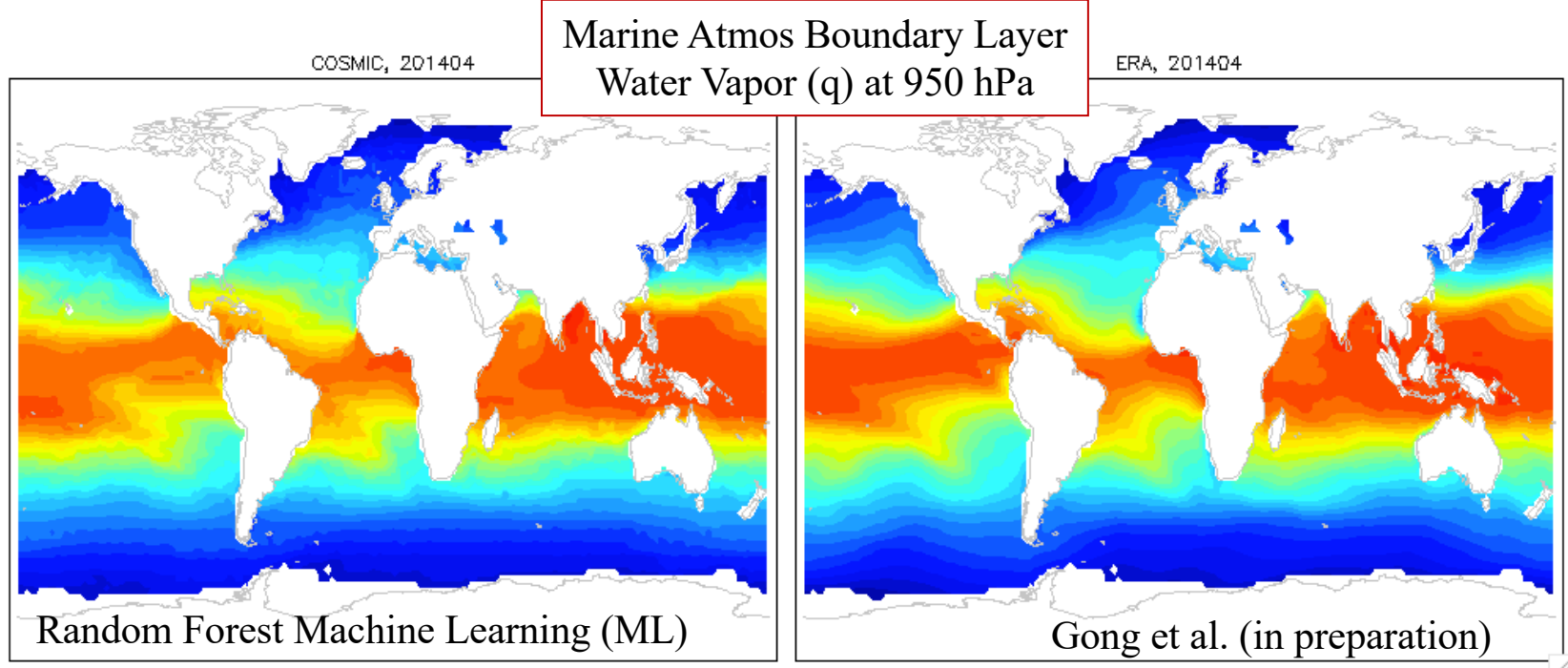
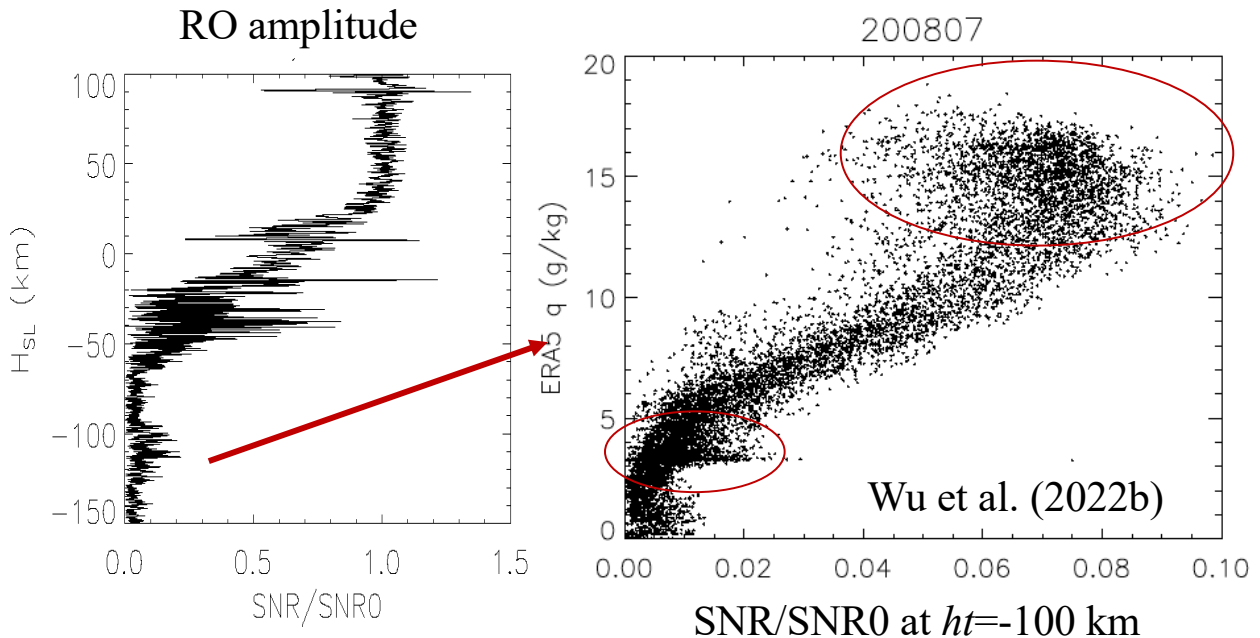
Comparison of **Level-2 atmPrf**
Sampling Statistics from Spire,
COSMIC-1 and COSMIC-2:

- Spire has generally lower but comparable sampling in PBL;
- Large fraction of SPIRE RO profiles reach 1km level;
- Monthly variability in SPIRE RO penetration (%) evident at 1km level (tropics and NH midlatitude) and 200m level (NH midlatitude and NH polar regions).

(Courtesy of M. Ganeshan)

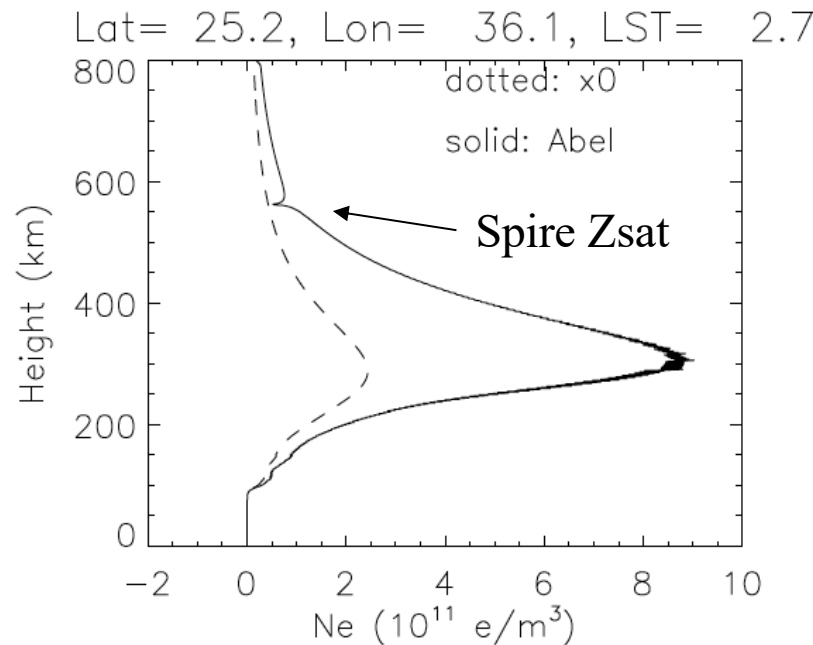
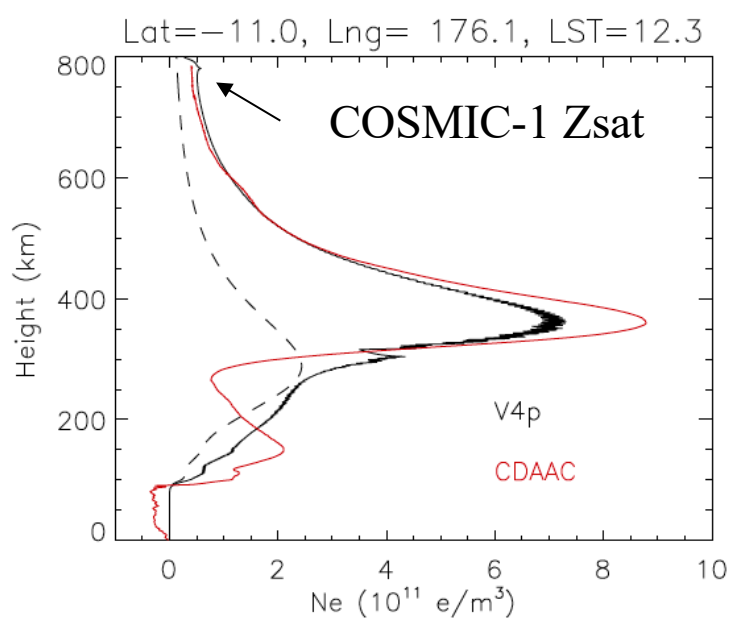


- Novel method to infer PBL water vapor (q) from GNSS-RO amplitude
- Benefit of global GNSS-RO sampling to study diurnal variations and polar regions

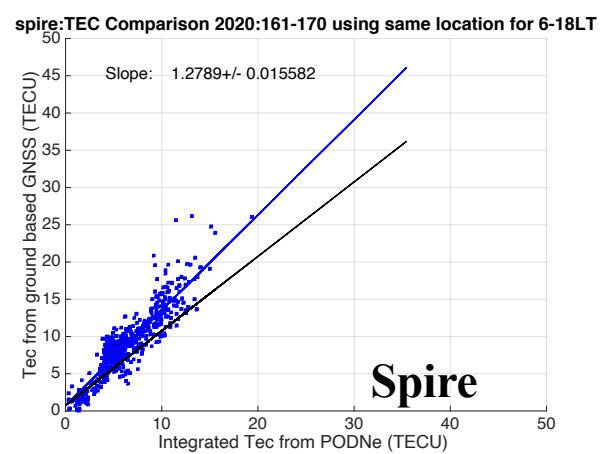
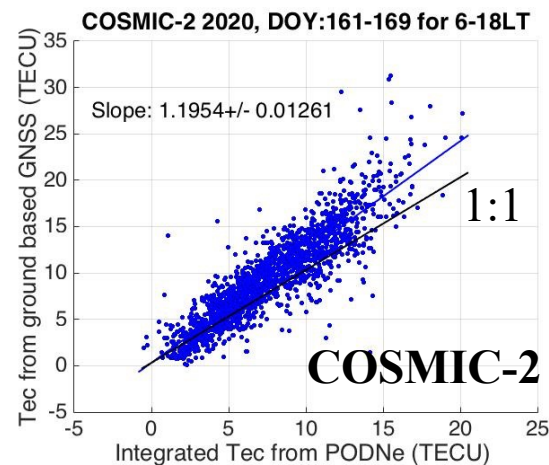
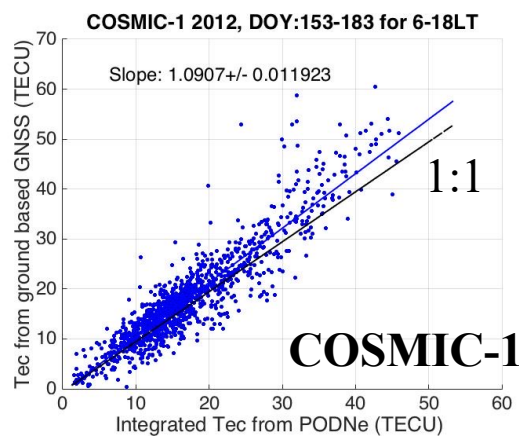




Ionospheric Sciences



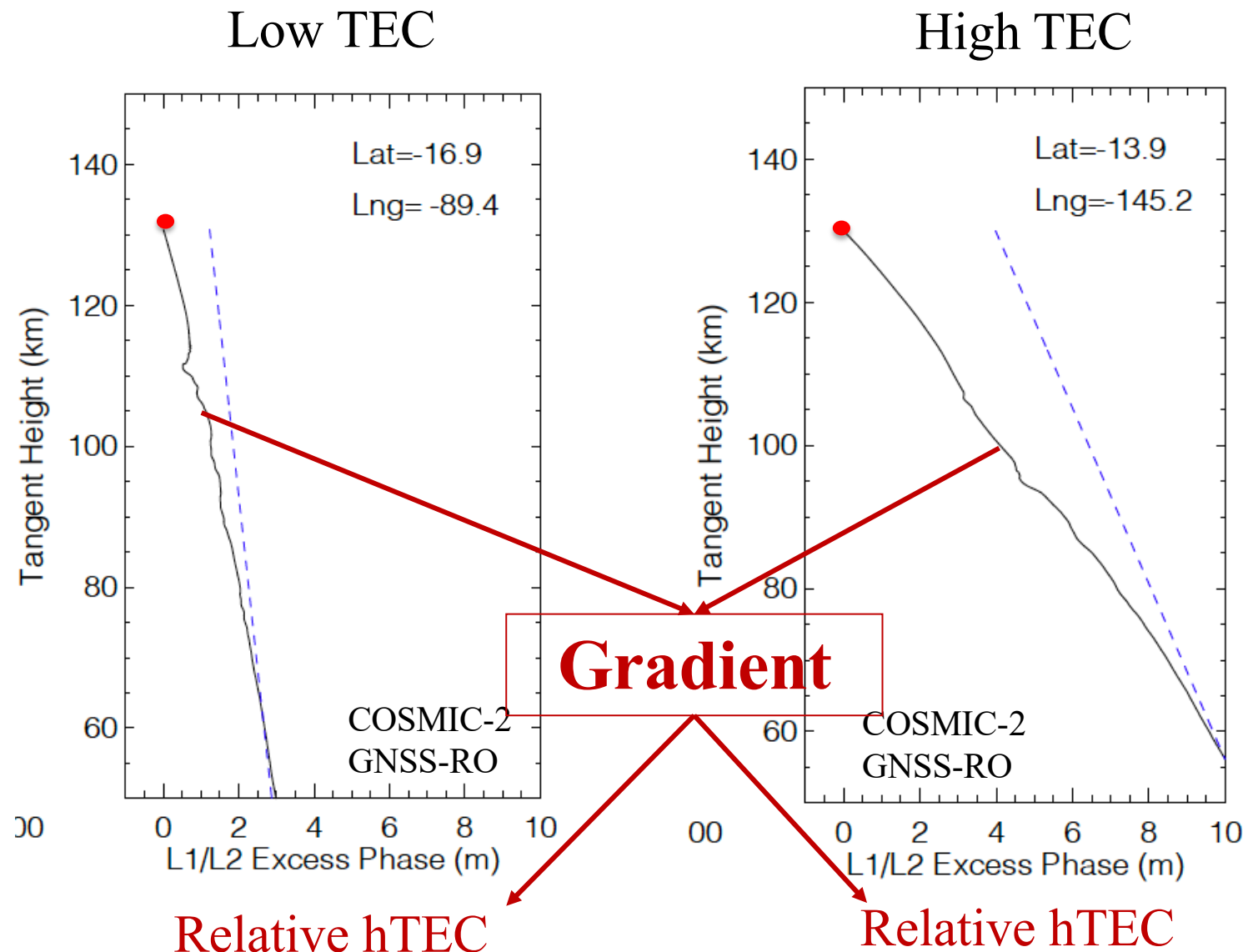
Comparisons with TEC from IGS Network



Under evaluation

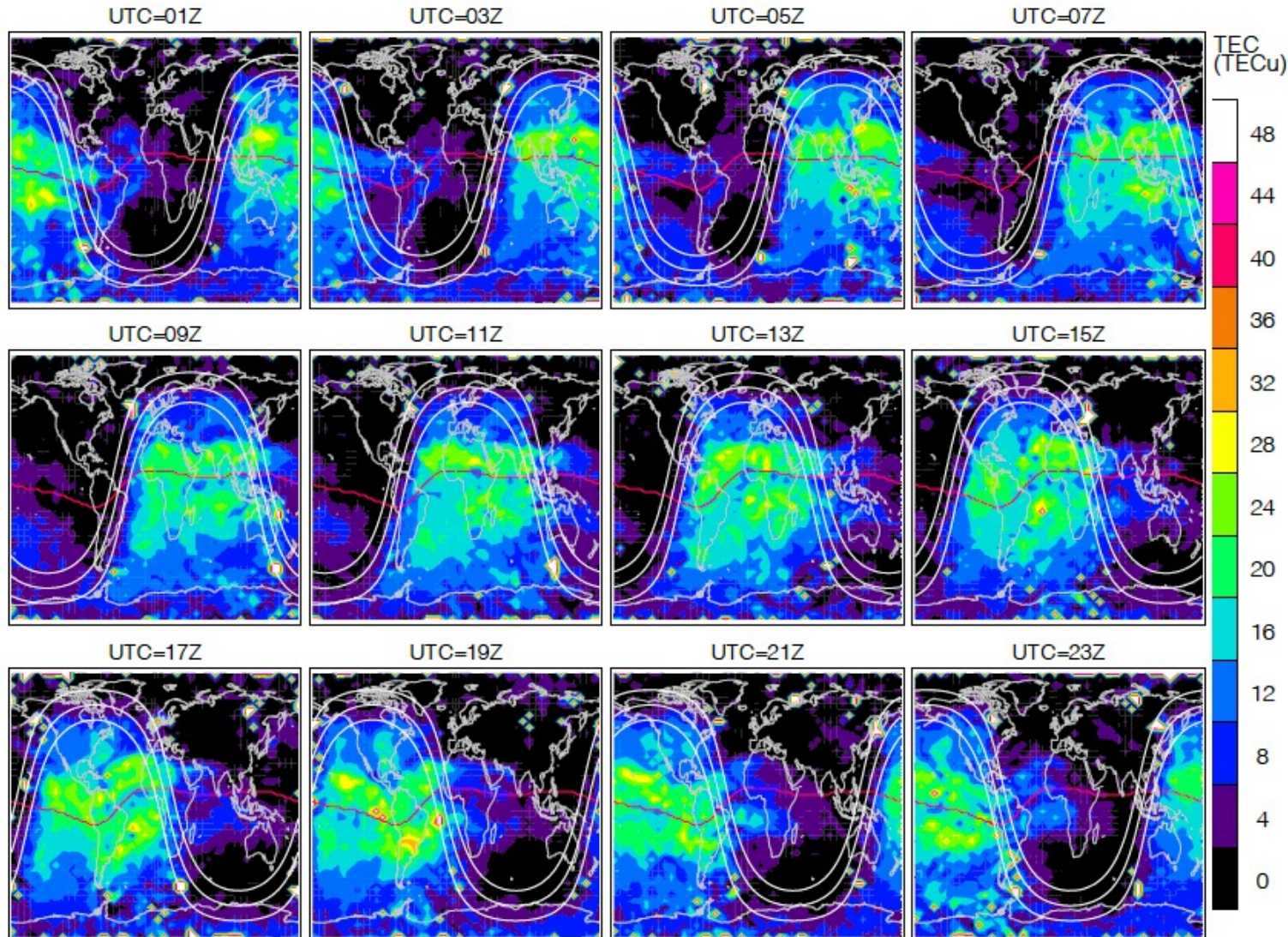


TEC Derived from GNSS-RO Gradient





Spire 2-Hourly TEC Maps from Jan 2022





References

- Angling, M. J., et. al. (2021). Sensing the ionosphere with the Spire radio occultation constellation, *J. Space Weather Space Clim.* 11 56, DOI: 10.1051/swsc/2021040
- Wu, D.L., Ionospheric S4 Scintillations from GNSS Radio Occultation (RO) at Slant Path. *Remote Sens.* 2020, 2(15), 2373; <https://doi.org/10.3390/rs12152373>
- Wu, D.L.; Emmons, D.J.; Swarnalingam, N. Global GNSS-RO Electron Density in the Lower Ionosphere. *Remote Sens.* 2022a, 14, 1577. <https://doi.org/10.3390/rs14071577>
- Wu, D.L.; Gong, J.; Ganeshan, M. GNSS-RO Deep Refraction Signals from Moist Marine Atmospheric Boundary Layer (MABL). *Atmosphere* 2022b, 13, 953. <https://doi.org/10.3390/atmos13060953>
- Wu, D.L., et al. (2023), Optimal Estimation Inversion of F-Region Electron Density from GNSS-POD Measurements: Part I. Algorithm and Data Reduction, in preparation.
- Swarnalingam, N., et al. (2023), Optimal Estimation Inversion of F-Region Electron Density from GNSS-POD Measurements: Part II. Validation of hmF2 and NmF2, in preparation.